Engineered Science
DOI: https://dx.doi.org/10.30919/es1568

# Thermosetting Behavior and Adhesive Application of Lac Terpene Acid under Solvent-Free Conditions

Shuaifei Yang,[1,2] Lanxiang Liu,[2,*] Hisham Essawy,[3] Qi Chen,[4] Juan Xu,[2] Jinju Ma,[2] Hong Zhang[1,2,*] and Chunhua Wu[1,*]

## Abstract

Lac terpene acid (LTA) is frequently discarded as industrial waste due to the significant challenges associated with its high-value utilization. In this work, the waste liquid from shellac saponification to obtain the LTA was investigated, and then the thermal property of LTA was investigated, and its application was developed. It was confirmed that LTA hydroxyl groups oxidize at 150 °C to form aldehydes/ketones, while its solidification at 225 °C primarily results from self-polymerization through esterification, yielding polymeric materials. Therefore, LTA as a high-performance thermosetting adhesive, capable of bonding a wide range of materials, is including metals, glass, wood, and paper. Notably, LTA achieves 12.25 MPa shear strength on metal substrates and demonstrates exceptional stability in harsh environments after heat curing. The study offers a theoretical and practical basis for the development and high-value utilization of LTA also provides a new reference for the study of terpene compounds.

*Keywords:* Lac terpene acid; Thermosetting adhesive; Solvent free; Stability; High-value utilization.
Received: 15 May 2025; Revised: 24 May 2025; Accepted: 28 May 2025.
Article type: Research article.

## 1. Introduction

Shellac is a natural resin secreted by lac insects,[1-3] which is commonly film-forming agent,[4,5] adhesive,[6] and sustained-release drug.[7] At present, it is often saponified in sodium hydroxide solution in industry, through salting out, filtration, bleaching, acid out, centrifugation, purification, drying and other processes to obtain high purity aleuritic acid ($C_{16}H_{32}O_5$).[8,9] In recent years, due to the sharp increase in the demand for aleuritic acid in the fields of flavors, fragrances and medicine, the discharge of the waste liquid from shellac saponification process (shellac waste liquid for short) after shellac resin extraction of aleuritic acid is also increasing, which raises environmental and recycling concerns that have attracted great attention from researchers and industry.

The treatment of lac wastewater commonly employs technologies such as sedimentation, thermal coagulation, electrolytic flocculation, UV-Fenton oxidation, hydroxyl radical oxidation, and biological methods. However, most of these technological analyses remain at the theoretical level, lacking support from specific experimental data, and there is still room for improvement in their practical applicability.[10] At present, the shellac waste liquid in the industry is generally dumped or incinerated, which not only seriously pollutes the environment, but also causes great waste of resources and has a negative impact on the economic benefits of shellac processing enterprises. There is an urgent need for the industry to find a suitable way to recycle shellac waste liquid and achieve its high-value recycling. In the preliminary work, researchers modified the waste liquid with chemical reagents such as polyvinyl alcohol, polymerized rosin glycidyl ester, epoxy, resulting in materials such as foam, hot melt adhesives, and resins.[11,12] Suchandra *et al*. used shellac waste liquid and

[1] *College of Materials and Chemical Engineering, International Joint Research Center for Biomass Materials, Southwest Forestry University, Kunming, Yunnan, 650224, China*
[2] *Chinese Academy of Forestry Institute of Highland Forest Science, Key Laboratory of Breeding and Utilization of Resource Insects of National Forestry and Grassland Administration, Yunnan Key Laboratory of Breeding and Utilization of Resource Insects, Kunming, 650233, China*
[3] *Department of Polymers and Pigments, National Research Centre, Dokki, Cairo, 12622, Egypt*
[4] *Hebei Technological Innovation Center for Volatile Organic Compounds Detection and Treatment in Chemical Industry, Hebei Chemical & Pharmaceutical College, Shijiazhuang, 050026, China*
**E-mail:* kmwuchunhua@163.com (C. H. Wu); kmzhh@hotmail.com (H. Zhang); lanxiangliu@outlook.com (L. X. Liu)

jute fiber to develop low-cost composite materials. However, the temperature increase showed some instability, mechanical tests indicate that the strength performance of this material needs improvement. The resin matrix exhibits significant thermal degradation at 80 ℃, and the composite fabrication process involves multiple complex processing steps, and the mechanistic evidence provided was limited.[6] The aforementioned research provides a potential avenue for the reuse of shellac waste liquid.[13] However, several challenges remain, including the mechanism of the modification process is not clear, the process is complicated, the cost is high, the material properties are low, and so on. It is still a great challenge to continuously explore the high-value utilization of the waste liquid from shellac saponification. Compared with raw materials such as lignin and tannic acid, lac terpenic acid exhibits higher reactivity and self-polymerization capability, superior water and chemical resistance, and lower process complexity. These advantages, along with its enhanced environmental friendliness, provide a unique pathway for the high-value utilization of shellac waste liquor.

A large amount of lac terpene acid (LTA) can be obtained from the shellac waste liquid by washing and refining.[14,15] After isolation and identification, LTA mainly contains about 70% by weight of jalaric acid and laccijalaric acid, laksholic acid, laccishellolic acid, shellolic acid and laccilaksholic acid are also present Fig. 1 (A).[16,17] Their chemical structure contains a large number of hydroxyl, carboxyl, aldehyde and carbon-carbon double bonds, which provide active sites for many chemical reactions and contribute to the formation of structurally diverse LTA derivatives and the preparation of novel functional materials. As for LTA itself, because its structure contains a variety of active functional groups, even without the addition of other substances, it has the potential to undergo various reactions such as esterification, etherification, oxidation under heating conditions.

Although the components of LTA have been isolated, purified and characterized, few studies have been reported on their chemical properties, especially their changes under heating conditions. In this work, shellac waste liquid was initially refined to obtain the LTA, and then thermal properties of the LTA were investigated at different temperatures, and its application in the field of hot melt adhesive or thermosetting adhesive was developed. A schematic diagram of the LTA reaction is shown in Fig. 1(B). Without the addition of any solvents or crosslinkers, an adhesive with superior properties can be synthesized by thermal self-polymerization using only LTA raw material. The prepared adhesive shows significant promise for applications in extreme conditions and maintains robust adhesive properties on various substrate materials, such as metallic, glass, wood, and paper. This research approach significantly reduces the cost of adhesive preparation, simplifies the production process, and provides clear mechanistic evidence and explanation, providing theoretical and practical basis for the development and utilization of high value LTA, and also provides a new reference for the research of terpene compounds.

## 2. Materials and methods

### 2.1 Materials

Sodium hydroxide, sodium chloride, petroleum ether, dichloromethane, tetrahydrofuran, imidazole, pyridine, 1,4-dioxane, and hydroxylamine hydrochloride were purchased from Guangdong Guanghua Technology Co. (Guangdong, China). Methanol, anhydrous ethanol, 95% ethanol, dimethyl sulfoxide, ethyl acetate, formic acid, potassium hydroxide, hydrochloric acid, and N,N-dimethylformamide were purchased from Tianjin Windship Chemical Reagent Technology Co. Acetone was purchased from Sichuan Xilong Science Co. (Tianjin, China). Ether was purchased from Chengdu Cologne Chemical Co. (Chengdu, China). All the reagents were chemically pure. The adhesives used in this study included: Item 1 is JL-6103C one-component high-temperature-resistant epoxy adhesive (Dong Hana Juli Adhesive Products Co., Ltd.); Item 2 is Seymour 8171 heat-curing adhesive (Shenzhen Seymour New Material Co., Ltd.). Shellac waste liquid was provided by Mojiang Senyuan Technology Co., Ltd. (Yunnan, China). The water used in this study was deionized water.

### 2.2 Refining of LTA

200 g of shellac waste liquid was placed in 2 L beater, and sulfuric acid at 18% by mass was added to adjust the pH of the solution to about 3 to precipitate the solid, then the precipitate was ultrasonicated with 0.8 L water for 20 min and left for 10 min, the upper liquid was poured off, and the solid was stirred repeatedly and washed for 5 times, the obtained solids were freeze-dried for 48 h and dried under vacuum conditions at 60 ℃ for 48 h to obtain the refined LTA, with a yield of about 48%.

### 2.3 Acid value measurement

The acid value of LTA was determined according to GB/T 8143-2008 of the Shellac Product Testing Standard. Weigh 0.3 g of the sample and put it into a 100 mL beaker, add 50 mL of 95% ethanol for ultrasonic dissolution and titrate with 0.1 $mol \cdot L^{-1}$ potassium hydroxide (KOH)-ethanol standard solution using a potentiometric titrator. The standard solution was prepared by dissolving 8 g of potassium hydroxide in a polyethylene container using 5 mL of deionized water. The solution was then diluted with 95% ethanol to a final volume of 1000 mL. After sealing, the solution was allowed to stand for 24 h, and the supernatant was carefully collected for later use. The endpoint of the titration was determined using a pH electrode, and the procedure was performed in triplicate to ensure accuracy and reproducibility. The blank control experiment was performed using 95% ethanol as the reference system. Without the addition of LTA samples, potentiometric titration was conducted with a 0.1 $mol \cdot L^{-1}$ KOH-ethanol standard solution to determine the background acid value of the solvent system. The acid value is calculated by the mass

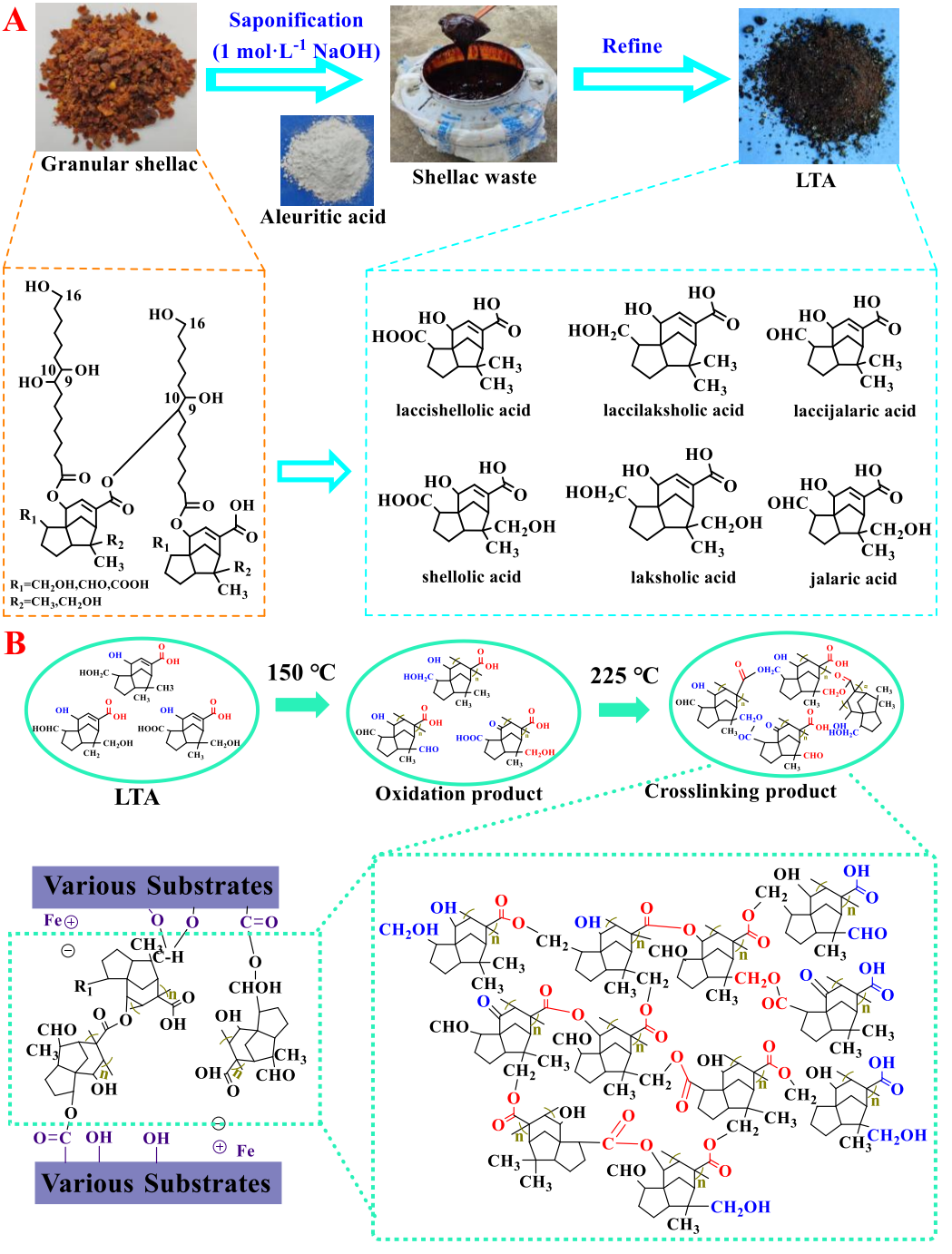


**Fig. 1:** (A) LTA production process and chemical structure of shellac resin and LTA, (B) Schematic diagram of LTA reaction under solvent-free heating and working principle of action under various substrates.

fraction of potassium hydroxide $X_1$ (mg KOH·g$^{-1}$), and the acid value is calculated by Eq. (1).

$$X_1 = \frac{(V_1 - V_0)C_1 * 56.11}{m_1} \quad (1)$$

where $X_1$ is the acid value of the sample material LTA (mg KOH·g$^{-1}$), $V_1$ is the volume of potassium hydroxide (KOH)-ethanol standard solution consumed by the sample (mL), $V_0$ is the volume of KOH-ethanol standard solution consumed by the blank group (mL), $C_1$ is the concentration of KOH-ethanol standard solution (mol·L$^{-1}$), 56.11 is the molar mass of KOH (g·mol$^{-1}$), and $m_1$ is the mass of the sample material LTA (g).

### 2.4 Measurement of hydroxyl value

According to the literature method,[18] 2 g of sample was weighed into a 250 mL round-bottomed flask, 50 mL of pyridine was added to dissolve, then 0.1 g of imidazole and 25 mL of acylating agent (V pyridine: V acetic anhydride = 4:1) were added to the system and placed in a water bath at 90 ℃ for 1 h. After cooling the system to room temperature, 50 mL of hydrolysate (V pyridine: V water = 2:1) was added to completely hydrolyze the unreacted acetic anhydride, then transferred to a beater for titration with 2 mol·L$^{-1}$ potassium hydroxide-ethanol standard solution using a potentiometric

titrator. The titration endpoint was determined using a pH electrode, when the end point was reached, the volume of titration solution consumed was recorded. The blank control was prepared without the addition of the raw material LTA, while all other experimental procedures and conditions remained the same as those of the sample tests. The hydroxyl value of the sample was calculated according to Eq. (2).

$$X_2 = \frac{(V_2 - V_2')C_2 * 56.11}{m_2} + X_1 \quad (2)$$

where $X_2$ is the hydroxyl value of the sample material LTA, the unit being mg KOH·g$^{-1}$; $V_2$ is the volume of KOH-ethanol standard solution consumed after complete hydrolysis of acetic anhydride in the blank sample, the unit being mL; $V_2$' is the volume of KOH-ethanol standard solution consumed after complete hydrolysis of the sample after acetylation, the unit being mL; $C_2$ is the KOH-ethanol standard solution, the unit being mol·L$^{-1}$; 56.11 is the molar mass of KOH, the unit being g·mol$^{-1}$; $m_2$ is the mass of the sample material LTA, the unit being g; $X_1$ is the acid value of the sample material LTA, the unit being mg KOH·g$^{-1}$.

### 2.5 Determination of the aldehyde value

Using the hydroxylamine hydrochloride method, the 0.3 g sample was accurately weighed and dissolved in 20 mL of N, N-dimethylformamide solution and then added to 10 mL of 2% (w/v) hydroxylamine hydrochloride aqueous solution. The mixed solution was allowed to react for 0.5 h at room temperature and then titrated with potassium hydroxide solution at a concentration of 0.2 mol·L$^{-1}$. The volume of solution consumed is recorded at the end of the titration. Meanwhile, the titration endpoint was determined using a pH electrode, the blank control was prepared without the addition of the raw material LTA, while all other experimental procedures and conditions remained consistent with those of the sample tests. The aldehyde group value is calculated according to Eq. (3): [19]

$$X_3 = \frac{(V_3 - V_3')C_3 * 56.11}{m_3} - X_1 \quad (3)$$

where $X_3$ is the aldehyde group value of the sample material LTA (KOH·g$^{-1}$), $V_3$ is the volume of the KOH-ethanol standard solution consumed by the sample (mL), $V_3$' is the volume of the KOH-ethanol standard solution consumed by the sample (mL), $C_3$ is the concentration of the KOH-ethanol standard solution (mol·L$^{-1}$), 56.11 is the molar mass of KOH (g·mol$^{-1}$), $m_3$ is the mass of the sample material LTA (g), and $X_1$ is the acid value of the sample material LTA (mg KOH·g$^{-1}$).

### 2.6 Characterization methods

Fourier transform infrared spectroscopy (FTIR): The structural characterization of LTA raw materials and samples, processed at different thermosetting temperatures and durations, was performed using a Tensor-27 Fourier Transform Infrared Spectroscopy (Netzsch, Germany). Functional group analysis was performed by using the potassium bromide pressed tablet method, with the FTIR spectra recorded over a wave number range from 4000 cm$^{-1}$ to 400 cm$^{-1}$, ensuring a comprehensive study of the molecular structure.

X-ray photoelectron spectroscopy (XPS): The surface elemental composition of the raw material LTA, as well as LTA products heated at 150 ℃ for 60 min and 225 ℃ for 60 min, was qualitatively and quantitatively analyzed using a PHI 5000 VersaProbe II X-ray photoelectron spectrometer (Japan). The analysis was performed under the operating conditions of 15 kV and 50 W, ensuring accurate characterization of the elemental distribution and chemical states on the material surfaces. The PHI5000 VersaProbe II X-ray photoelectron spectrometer (Japan) was used for the analysis of the surface elements of the sample under the operating conditions of 15 kV and 50 W.

Thermogravimetric (TG): TG analysis of the raw material LTA was performed using a STA 2500 synchronous thermal analyzer (Netzsch, Germany). This instrument was used to evaluate the thermal stability and decomposition behavior of the material under controlled temperature conditions. During the test, 5-8 mg samples were placed in a special alumina ceramic crucible, and high-purity nitrogen with a purity of ≥ 99.99% was used as the protective atmosphere and purge gas. The gas flow rate was 50 mL·min$^{-1}$, the purge gas flow rate was 20 mL·min$^{-1}$, and the heating rate was 10 ℃·min$^{-1}$. The measurement temperature range was 25-600 ℃, and the cooling method adopted was automatic cooling.

Dynamic Mechanical Analysis (DMA): The DMA test for LTA was conducted using the Q800 instrument (TA, American). The test used a three-point bending mode with a selected frequency of 5 Hz. The temperature range for the test was from 25-250 °C, with a heating rate of 5 °C·min$^{-1}$. The specimen dimensions were 40 mm × 10 mm × 1.5 mm, made of poplar wood.

Differential Scanning Calorimetry (DSC): Thermal transitions were analyzed using a STA2500 Thermal Analyzer (Netzsch, Germany). Samples weighing approximately 10 mg were sealed in the aluminum crucible and subjected to a temperature range of -30 °C to 300 °C at a heating rate of 10 ℃·min$^{-1}$ under a high-purity nitrogen atmosphere. The protective and purge gas flow rates were set at 50 mL·min$^{-1}$ and 80 mL·min$^{-1}$, respectively.

### 2.7 Rheological tests

The raw material LTA was formed into a circular sample with a diameter of 25 mm and a thickness of 1 mm, which was then placed on a plate mold. The rheological properties of LTA were evaluated using a TA Discovery HR-2 rheometer (TA Instruments, USA). This instrument was used to characterize the flow and deformation behavior of the material under controlled conditions. The flow temperature ramp mode was selected to test the viscosity change with temperature. The pre-test stability time was 2 min, the gap height of the sample on the mold during the test was 1000 μm, the gap height does not

affect the results, the heating rate was 5 ℃·min$^{-1}$, according to the method specified in GB/T 33061.10, the shear rate was set at 10 s$^{-1}$ and the test temperature was 25-300 ℃. The oscillation temperature ramp mode was selected to test the variation of the energy storage modulus with temperature. The oscillation temperature ramp mode shows that the oscillation time is 2 min, the gap height of the sample on the mold during the test was 1000 μm, the heating rate was 5 ℃·min$^{-1}$, the pressure is 8.5 Pa, and the shear rate is 10 s$^{-1}$.

### 2.8 Determination of the shear strength of the LTA adhesive

The heating process of the adhesive consists of four main steps: preheating, coating, heat curing, and cooling. To evaluate the influence of temperature and time on the bonding properties, the experiments were conducted according to the national standard GB/T 7124-2008 (Adhesives-determination of tensile lap-shear strength of rigid-to-rigid bonded assemblies) and ASTM D1002 (Apparent shear strength of single-lap-Joint adhesively bonded metal specimens by tension loading). Specifically, 3 g of LTA was preheated on a constant temperature hot plate with a digital readout at 110 °C for 5 min until it became liquid. The liquid LTA was then applied to substrates such as stainless steel, aluminum sheet, and tempered glass, with a coating area of 12.5 mm × 25 mm and an adhesive layer thickness of 0.2 mm. A pressure of 1.38 MPa per unit area was applied to the metal substrate within the bond area. The bonded substrates were then placed in an oven and cured at various temperatures for specified periods of time. After curing, the samples were removed from the oven and allowed to cool to room temperature for further analysis. An AGX-V-5 kN universal testing machine was used to measure the shear strength.[20] The distance between the test specimens was 90 mm and the speed was 10 mm·min$^{-1}$. The shear strength (MPa) is calculated by dividing the ultimate load (N) by the shear area (mm$^2$).

### 2.9 Stability test of LTA thermoset products

The LTA bonded stainless steel substrates were subjected to hot curing in an oven at different temperatures and durations. After curing, the samples were immersed in 0.5 L of various solutions, including 0.1 mol·L$^{-1}$ HCl, 0.1 mol·L$^{-1}$ NaOH, 1 wt% NaCl, petroleum ether, deionized water, and 95 °C water for 24 h. After immersion, the samples were removed, thoroughly rinsed with deionized water, and dried at room temperature. The shear strength of the samples was then measured according to the procedure described in Section 2.8.

### 2.10 Statistical Analysis

All experiments were conducted in triplicate unless otherwise specified, with data expressed as mean ± standard deviation. Statistical analyses were performed using SPSS Statistics 17.0 software, employing Duncan's multiple-range test for post-hoc comparisons. * is p value ≤0.05, **is p value ≤0.01, *** is p value ≤0.001.

## 3. Results and discussion

### 3.1 Basic physicochemical properties of the LTA

The solubility test results showed that LTA has a solubility greater than 100 mg·mL$^{-1}$ in N, N-dimethylformamide, pyridine, methanol, ethanol, and 0.1 mol·L$^{-1}$ sodium hydroxide solution. It was soluble in tetrahydrofuran, dimethyl sulfoxide and 1,4-dioxane with a solubility greater than 60 mg·mL$^{-1}$. But the LTA was insoluble in water, 0.1 mol·L$^{-1}$ hydrochloric acid solution, ethyl acetate, methylene chloride, acetone, ether, and other solvents. As shown in Table 1, the acid value of LTA was 99.72 mg KOH·g$^{-1}$, the hydroxyl group value was 274.23 mg KOH·g$^{-1}$, the aldehyde value was 13.58 mg KOH·g$^{-1}$, the ratio of carboxyl group, hydroxyl group and aldehyde group was about 7.3: 20.2: 1, and the LTA pH value of 0.1 mol·L$^{-1}$ was 5.69. The structure of LTA is basically consistent with that reported in the literature, and it is a mixture of different lac terpene acid.

### 3.2 Thermal properties of the LTA

Initially, the rheological properties of LTA were systematically investigated under temperature-dependent conditions using two distinct measurement modes. The temperature-viscosity test results in Fig. 2(A) shows that the viscosity of LTA generally changes in two stages with increasing temperature. In the first stage, the viscosity of LTA decreased sharply with increasing temperature. When the temperature reached about 200 ℃, the viscosity of LTA remained at about 0.04 Pa·s, indicating that the substance was liquid.[21,22] In the second stage, as the temperature continued to increase from 200 ℃ to 300 ℃, the viscosity of the substance in this temperature range gradually increased progressively to about 5.81 Pa·s, indicating that the chemical reaction of LTA produces a substance with higher viscosity.[23,24] In addition, the temperature-modulus test results were shown in Fig. 2(B). As the temperature increased from room temperature to 132 ℃, the loss modulus and energy storage modulus continued to decrease, and the loss modulus was always larger than the energy storage modulus, indicating that LTA was liquid and that mainly viscous deformation occurred in this temperature range,[25] the energy storage modulus shows an increasing trend in the temperature range of 105-132 ℃, indicating that polymerization of carbon-carbon double bonds may have occurred within the LTA molecules.[26,27] In the temperature range of 132-225 ℃, the energy storage modulus and the loss modulus of LTA were the same, indicating that the structure of the raw material collapsed and a phase transition occurred, at which time LTA was a gel-like semi-solid.[28] When the temperature was higher than 225 ℃, the energy storage modulus of LTA was larger than the loss modulus, indicating that the chemical reaction of LTA was completed and a solid substance was formed.[29]

The weight loss behavior of LTA as temperature increased was largely consistent with the findings from the rheological tests. As shown in Fig. 2(C), LTA started to lose weight from about 230 ℃, and the weight loss rate reached the maximum

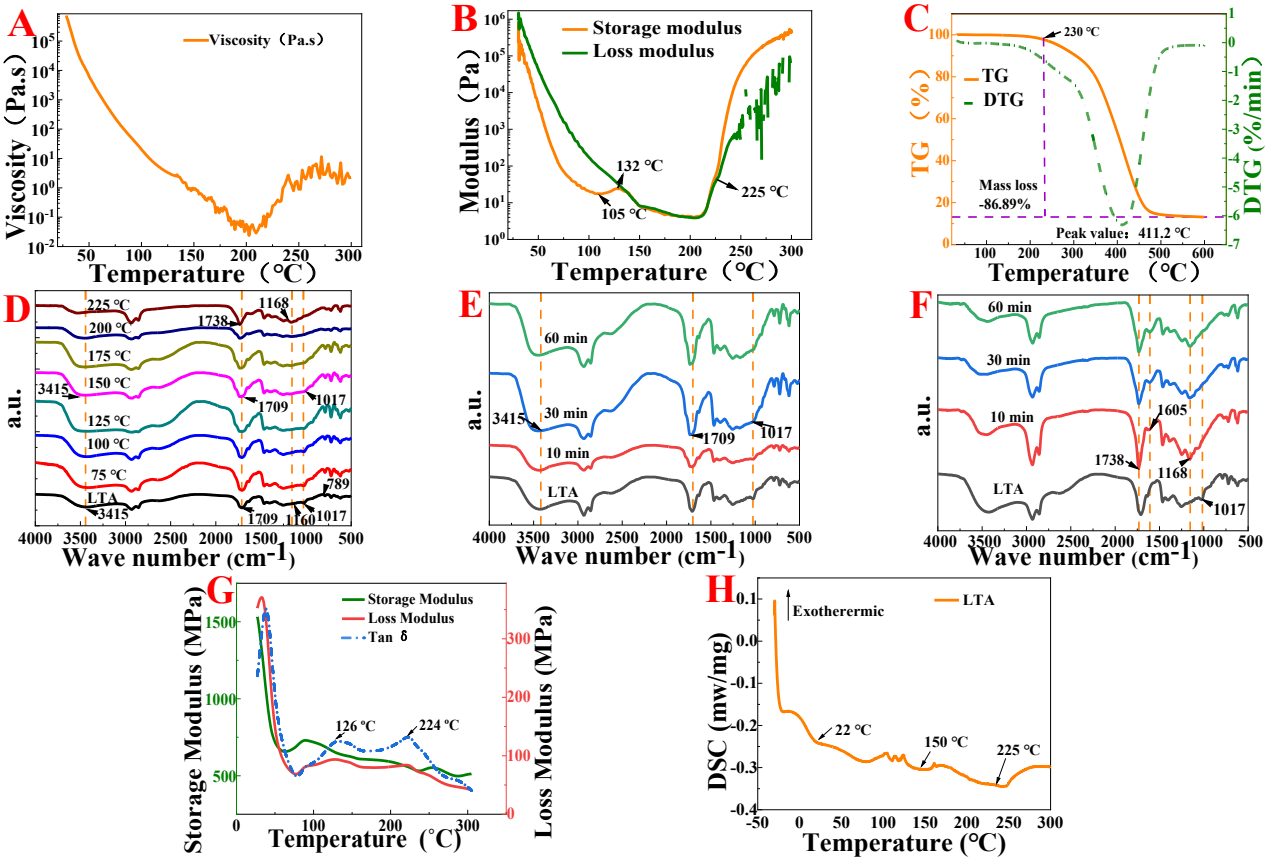


**Fig. 2:** (A) Temperature-viscosity test diagram of LTA, (B) Temperature-modulus test diagram of LTA, (C) TG and DTG Diagrams of LTA, (D) FTIR Diagram of LTA heating products at different temperatures in 60 min, (E) at 150 ℃ with different time, (F) at 225 ℃ with different time, (G) The DMA curves of LTA illustrate the variation of modulus with temperature at different reaction temperatures, and (H) Temperature-DSC test diagram of LTA.

**Table 1:** Basic physicochemical properties of the LTA.

| | Acid (mg KOH·g$^{-1}$) | Hydroxyl (mg KOH·g$^{-1}$) | Aldehyde (mg KOH·g$^{-1}$) | pH |
|---|---|---|---|---|
| Index | 99.72±4.51 | 274.23±2.10 | 13.58±3.03 | 5.69±0.14 |

value at 411 ℃. After that, the thermogravimetric rate started about 230 ℃, and the weight loss rate reached the maximum value at 411 ℃. After that, the thermogravimetric rate started to slow down and finally kept its mass unchanged after about 490 ℃, at which time the weight loss of LTA was about 86.89%.

To study the structure of LTA heating products at different temperatures, LTA was heated at 75 ℃, 100 ℃, 125 ℃, 150 ℃, 175 ℃, 200 ℃and 225 ℃ for 60 min, respectively, and then the products were characterized by infrared spectroscopy. As shown in Fig. 2(D), the LTA mainly had stretching vibration absorption peaks caused by -OH at 3415 cm$^{-1}$ and stretching vibration absorption peaks caused by -C=O and -C-O-C in carboxyl or ester groups at 1709 cm$^{-1}$ and 1160 cm$^{-1}$, respectively. And the stretching vibration absorption peak caused by the -C-O bond in the hydroxyl group at 1017 cm$^{-1}$.[13,30,31] When LTA was reacted at 75 ℃, 100 ℃, and 125 ℃ for 60 min, the absorption profile was similar to the raw material, indicating that there was no obvious chemical reaction in LTA at relatively low temperatures. When LTA was reacted at 150 ℃, 175 ℃ and 200 ℃ for 60 min, the absorption peaks of the products at 3415 cm$^{-1}$ and 1017 cm$^{-1}$ disappeared or became weaker, while the absorption peaks at 1709 cm$^{-1}$ increased in intensity and broadened, indicating that the hydroxyl group of LTA may be oxidized to aldehydes or ketones. The absorption peak of the product of LTA heated at 225 ℃ increased in intensity at 1738 cm$^{-1}$, a prominent absorption peak was observed of the C-O-C stretching vibration at 1168 cm$^{-1}$, indicating that a large number of ester groups were formed at this time.

To explore LTA alterations under high temperature, the fixed heating temperatures were 150 ℃ and 225 ℃ respectively, and the influence of heating time on LTA was investigated. As shown in Fig. 2(E), compared with LTA raw materials, the absorption peaks of LTA products remained unchanged after heating at 150 ℃ for 10 min, while the infrared absorption peaks of LTA products were basically the same after extending the heating time to 30 min and 60 min. their absorption peaks at 3415 cm$^{-1}$ and 1017 cm$^{-1}$ were weakened. However, the absorption peak at 1709 cm$^{-1}$

increased in intensity and broadened, indicating that part of the hydroxyl group of LTA may be oxidized to aldehydes or ketones at this time. However, Fig. 2(F) shows that when LTA was heated at 225 ℃ for 10 min, the absorption peak at 1738 $cm^{-1}$ and 1605 $cm^{-1}$ increased in sharper and more intense, while a C-O-C stretching vibration absorption peaks appeared at 1168 $cm^{-1}$. These results clearly show the formation of an ester absorption peaks, indicating that the increase in temperature is conducive to shortening the self-polymerization time of LTA. [32]

Fig. 2(G) In the DMA analysis of LTA at different temperatures, the Tan δ curve showed a peak at 126 ℃, indicating molecular relaxation at this temperature. This relaxation is likely due to the polymerization of carbon-carbon double bonds and changes in the degree of cross-linking within the LTA molecules, which is consistent with the upward trend in the energy storage modulus observed in the temperature range of 105–132 ℃ in the rheological tests. In addition, a peak at 224 ℃ indicates a phase transition, likely caused by an esterification reaction within the LTA molecules, leading to an increased degree of cross-linking and a transition from a gel state to a solid state. This finding was consistent with the experimental thermal cur temperature of LTA at 225 ℃ and the rheological test results, which showed that the energy storage modulus exceeded the energy dissipation modulus at 225 ℃. In Fig. 2(H), the DSC analysis revealed that the glass transition temperature (Tg) of LTA was 22 ℃. The material exhibited distinct endothermic peaks at 150 ℃ and 225 ℃, further confirming the occurrence of oxidation and esterification reactions during the heating process. Taken together, these observations highlight the thermal and structural evolution of LTA during the curing process.

To further characterize the products of LTA at different temperatures, we performed XPS characterization of the reaction products of LTA heated at 150 ℃ and 225 ℃ for 60 min respectively. It can be seen from Fig. 3 that LTA and the products at the two heating temperatures were mainly composed of carbon and oxygen elements. The content of carbon and oxygen elements in the crude LTA was basically the same as that in the products at 150 ℃, but the content of C=O group in the products at 150 ℃ increased by about 9%, indicating that the oxidation reaction is mainly caused by the hydroxyl group in LTA at this temperature.[33] The carbon and oxygen contents of the products heated at 225 ℃ were comparable to those of the raw LTA and the products heated at 150 ℃. However, a significant increase was observed in the C=O group content, which increased from 42.31% to 49.21% compared to the raw LTA, and in the C-O group content, which increased from 48.37% to 50.79% compared to the 150 ℃ product. In addition, the C-O:C=O ratio increased from 0.93 to 1.03 compared to the 150 ℃ product. These results indicate the formation of a substantial number of ester groups at 225 ℃. The analysis results of XPS were basically consistent with the characterization results of FTIR, indicating that when LTA was heated at 150 ℃ for 60 min, there is air around it. Due to the rich hydroxyl functional groups in its molecular structure, it is highly prone to oxidation reactions, the oxidation of hydroxyl group to aldehydes or ketones mainly occurrs, while the esterification reaction mainly occurrs at 225 ℃, resulting in self-polymerization to produce new polymer products.[34,35]

### 3.3 Adhesive properties of the LTA

According to the thermal properties of LTA, six temperature nodes such as 150 ℃, 175 ℃, 195 ℃, 215 ℃, 225 ℃ and 235 ℃ were selected as representative to investigate the influence of LTA thermosetting at different temperatures for 10 min, 30 min and 60 min on the adhesion to stainless steel substrate. As shown in Fig. 4, when the thermosetting temperature was 150 ℃ and the curing time was 10 min and 30 min, the shear strength of the product was maintained at 1.89 MPa and 1.98 MPa, and when the time was extended to 60 min, the shear strength was increased to 5.56 MPa. LTA can be used as an adhesive in different temperature ranges and can be used to bond paper, wood, glass, and metal. When the thermosetting temperature was 175 ℃ and 195 ℃ and the curing time was 10 min, the shear strength of the obtained product was only 1.93 MPa and 1.95 MPa, but when the time was extended to 30 min, the shear strength was increased to 9.37 MPa and 10.24 MPa, respectively, and did not change with time. The high shear strength of 8.87 MPa, 10.38 MPa and 10.71 MPa was obtained after heating for only 10 min at the high thermosetting temperature of 215 ℃, 225 ℃ and 235 ℃, and the adhesive performance was strong and reliable.

As shown in Fig. 4(E) and (F), the adhesion strength of LTA was evaluated on different substrates and commercial adhesives. The results showed that LTA exhibited strong adhesion strength on various substrates such as stainless steel, aluminum, tempered glass, PP, bamboo, wood and paper, with adhesion strengths of 12.25 MPa, 7.46 MPa, 6.81 MPa, 2.42 MPa, 2.49 MPa, 2.35 MPa, and 0.25 MPa, respectively. The enhanced bonding effect of LTA on metals may be due to metal coordination or electrostatic action between LTA and the metal surface. In order to prevent thermal degradation of non-temperature-resistant substrates at 225 ℃, a lower heat curing temperature was chosen, and its adhesion strength was selected. LTA adhesive and commercial adhesives item 1 and item 2 selected stainless steel substrate adhesion performance control shows that the shear strength of LTA exceeds the commercially available adhesives, LTA in the metal substrate shows superior adhesion performance, its shear strength shows a statistically significant difference from that of other substrates, which may be due to the LTA adhesives contain a large number of hydroxyl carboxyl and other functional groups in the high temperature highly esterified cross-linking to form a network structure at high temperature and the metal coordination or chelation with the metal surface.[36-38]

In practical applications, adhesives are frequently required to endure extreme environmental conditions, including exposure to water, seawater, acids, alkalis, and organic solvents. To assess the bonding properties of LTA with

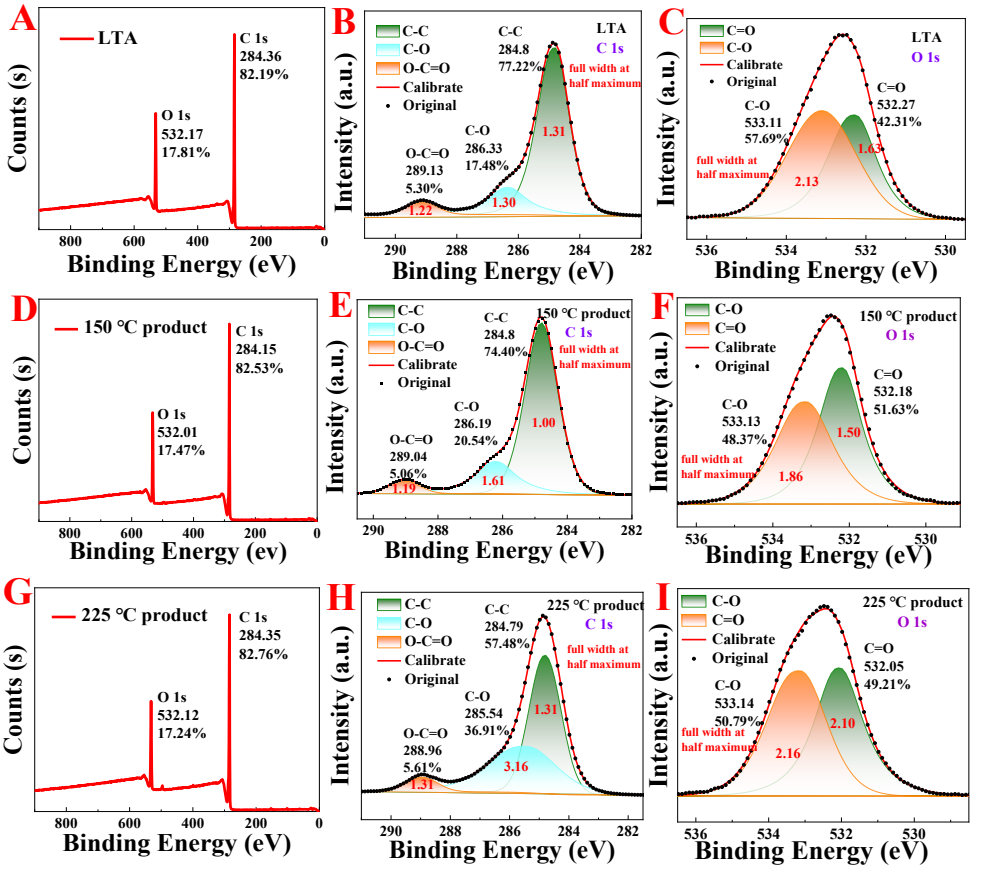


**Fig. 3:** (A) XPS Survey spectrum, (B) High-resolution spectra of C 1s and (C) High-resolution spectra of O 1s of the LTA, (D) XPS Survey spectrum, (E) High-resolution spectra of C 1s and (F) High-resolution spectra of O 1s of the reaction product of LTA was heated at 150 ℃ for 60 min, (G) XPS Survey spectrum, (H) High-resolution spectra of C 1s, and (I) High-resolution spectra of O 1s of the reaction product of LTA was heated at 225 ℃ for 60 min.

stainless steel substrate under various conditions, this study bonded LTA to stainless steel at temperatures of 150 ℃, 195 ℃, and 225 ℃ for 60 min. Subsequently, the bonded specimens were immersed in hydrochloric acid, sodium hydroxide, saline solution, petroleum ether, water， and 95 ℃ water for 24 h. The bonding stability was then evaluated through shear strength testing.

As shown in Fig. 5, the experimental findings reveal that the shear strength of the LTA-bonded steel substrate significantly decreases after 24 h of immersion in various solvents at 150 ℃, particularly in alkaline environments. This suggests that the polymerization products formed at this temperature exhibit poor stability under extreme conditions. When bonded at 195 ℃, the LTA showed minimal strength reduction after 24 h in water but experienced slight decreases in strength when exposed to acid, alkali, saline solution, and petroleum ether. In contrast, the LTA bonded at 225 ℃ maintained a stable shear strength of approximately 12.25 MPa after 24 h in various solvents. The adhesion strength showed no significant change after immersion in various solvents, with no statistically significant difference observed ($p>0.05$). This indicates that the polymerization products formed at this temperature possess superior stability.[20,39,40] This enhanced stability was likely due to the higher temperature promoting the formation of additional ester groups in the LTA, resulting in a cross-linked polymer structure that improves the material's hydrophobicity and chemical resistance. These properties make LTA adhesive highly promising for applications in harsh environments, such as those involving strong acids, strong alkalis, and marine conditions. For instance, in marine engineering, chemical processing equipment, and industrial machinery that require long-term exposure to aggressive media, LTA adhesives can serve as high-performance bonding materials, offering exceptional durability and reliability.[41-43]

## 4. Conclusion

The effluent generated from shellac deep-processing varies widely in composition and pollutant content due to differences in production batches and factory processes. Currently, this pollutant-rich effluent is underutilized as a resource, and research on shellac effluent remains limited. In this study, the waste liquid was first purified to remove impurities, resulting in refined LTA raw material. Analysis of its physical properties and chemical structure revealed that LTA contains active functional groups such as hydroxyl, aldehyde, and carboxyl, highlighting its potential for high-value utilization.

LTA exhibits temperature-sensitive behavior. Rheological

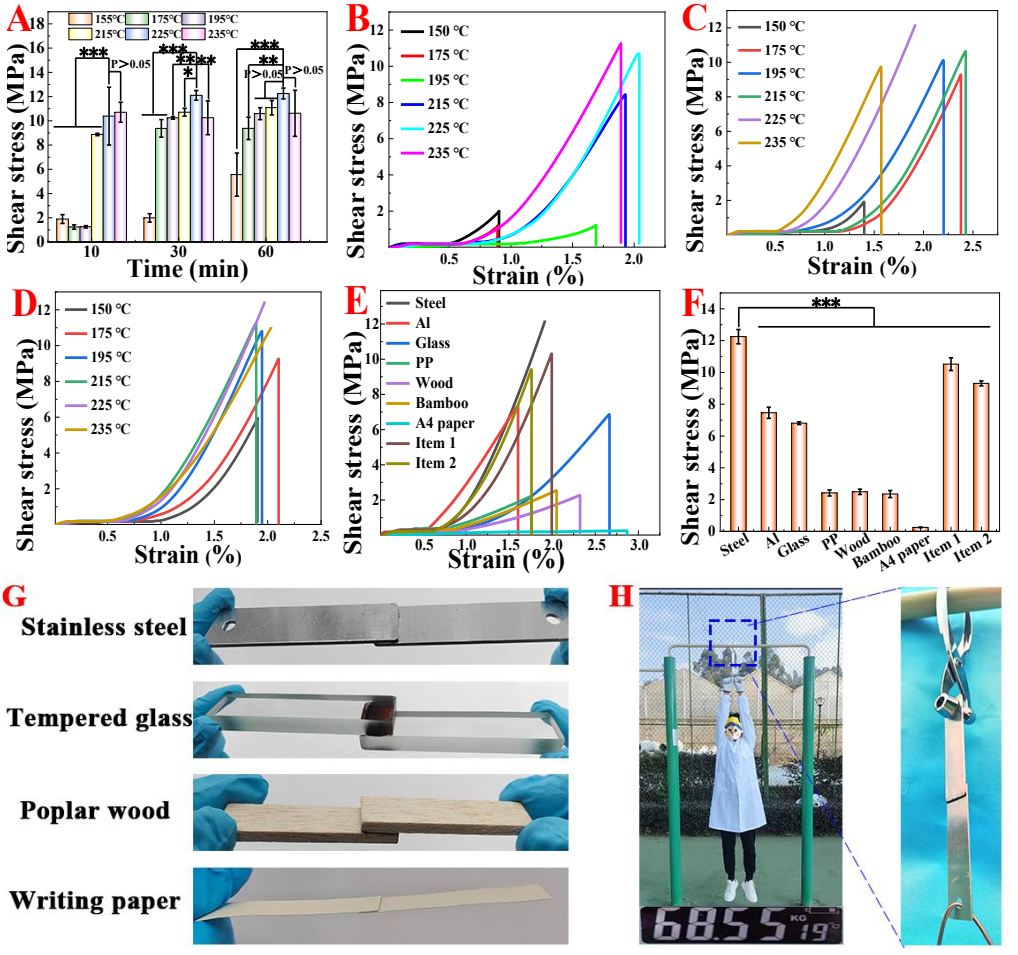


**Fig. 4:** (A) The change of the adhesive lap-shear of LTA at different temperatures with time. Adhesive curves of LTA adhesive to stainless steel by the lap-shear test at different curing time of (B) 10 min, (C) 30 min, (D) 60 min; (E) Adhesive curves and (F) summary of adhesive strength of LTA adhesive on different substrates and various commercially available adhesives on stainless steel by the lap-shear test. The curing temperature of stainless steel, aluminum, glass, item 1 and item 2 was 225 °C for 60 min, and the curing temperature of bamboo and poplar was 190 °C for 20 min, and the curing temperature of PP and A4 paper was 120 °C for 20 min; (G) Photos of bonding different substrates; (H) Outdoor photographs and partial magnification of bonded substrates. LTA-bonded stainless-steel substrates supported loads exceeding 68 kg.

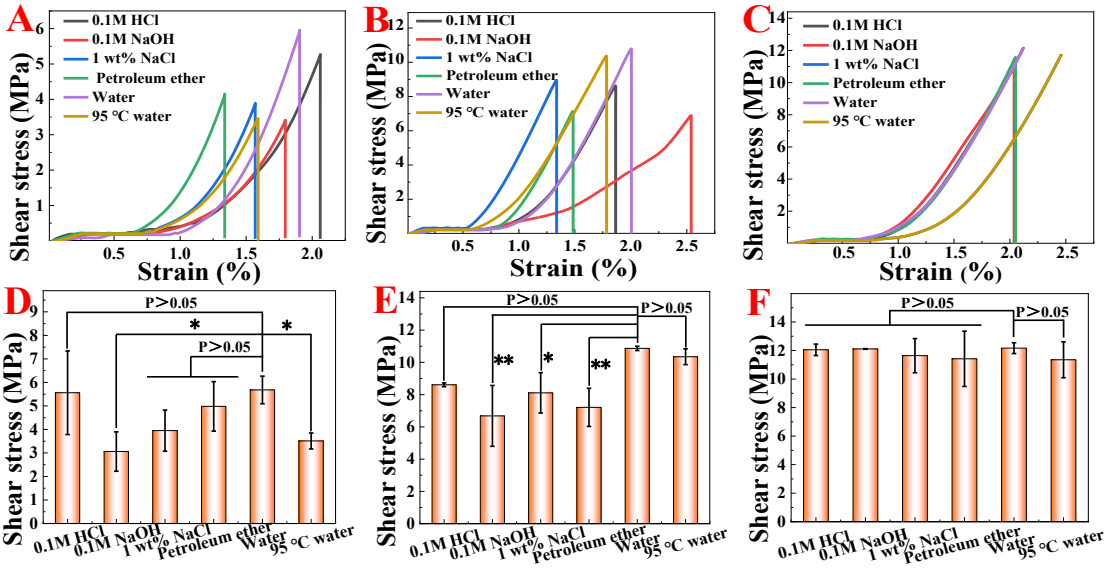


**Fig. 5:** Adhesion curves by the lap-shear test of LTA adhesive to stainless steel at (A) 150 °C, (B) 195 °C and (C) 225 °C for 60 min and soaked in different solutions for 24 h; Summary of adhesion strength of LTA adhesive to stainless steel at (D) 150 °C, (E) 195 °C and (F) 225 °C for 60 min and soaked in different solutions for 24 h.

and DMA tests indicate that cross-linking of carbon-carbon double bonds occurs at about 126 °C, while curing reactions occur at about 225 °C. Infrared and XPS analyses further show that the oxidation of hydroxyl groups to aldehyde groups occurs at about 150 °C, and esterification cross-linking reactions at about 225 °C to produce polymers that were insoluble in most solvents. After heat curing, LTA exhibits excellent adhesive properties, allowing it to bond to various substrates, including metals, glass, wood, and paper, at temperatures tailored to the specific requirements of each material. With a remarkable bond strength to metal exceeding 12.25 MPa, LTA shows promise for industrial adhesive applications.

LTA adhesives exhibit exceptional stability in harsh environments only after thermal curing, while showing some instability below the thermal curing temperature. In addition, the variability of production batches of shellac waste liquid and the high cost of recovery pose challenges to its widespread use. However, in applications where stringent adhesive performance and stability were not required, LTA shows promise for industrial adhesive applications as a solvent-free, heat-curable, waterproof, and tough adhesive. Its advantages in industrial manufacturing and environmental sustainability underscore its potential for wider adoption and high-value utilization.

**Acknowledgment**

The study was supported by Yunnan Fundamental Research Projects (No.202301AT070180), the National Natural Science Foundation of China (32160414, 32460369), the International Joint Research Center for Biomass Materials (Southwest Forestry University, No.20231102, No.2023-GH12), the 111 Project (D21027), and supported by the Open Fund of Hebei Technological Innovation Center for Volatile Organic Compounds Detection and Treatment in Chemical Industry(No. ZXJJ20240103). The authors express sincere gratitude to everyone who participated in this research.

**Conflict of Interest**

There is no conflict of interest.

**Supporting Information**

Not applicable.

**References**

[1] J. Gao, K. Li, J. Xu, W. Zhang, J. Ma, L. Liu, Y. Sun, H. Zhang, K. Li, Unexpected Rheological Behavior of a Hydrophobic Associative Shellac-Based Oligomeric Food Thickener, *Journal of Agricultural and Food Chemistry*, 2018, **66**, 6799-6805, doi: 10.1021/acs.jafc.8b01148.

[2] L. Liu, X. Li, G. Dong, H. Zhang, Y. Tao, R. He, J. Xu, J. Ma, B. Tang, B. Zhou, Bioinspired Natural Shellac Dressing for Rapid Wound Sealing and Healing, *ACS Applied Materials & Interfaces*, 2023, **15**, 43294-43308, doi: 10.1021/acsami.3c06734.

[3] N. Thombare, S. Kumar, U. Kumari, P. Sakare, R. K. Yogi, N. Prasad, K. K. Sharma, Shellac as a multifunctional biopolymer: A review on properties, applications and future potential, *International Journal of Biological Macromolecules*, 2022, **215**, 203-223, doi: 10.1016/j.ijbiomac.2022.06.090.

[4] H. Bar, H. Bianco-Peled, The unique nanostructure of shellac films, *Progress in Organic Coatings*, 2021, **157**, 106328, doi: 10.1016/j.porgcoat.2021.106328.

[5] Y. Yuan, N. He, Q. Xue, Q. Guo, L. Dong, M. H. Haruna, X. Zhang, B. Li, L. Li, Shellac: A promising natural polymer in the food industry, *Trends in Food Science & Technology*, 2021, **109**, 139-153, doi: 10.1016/j.tifs.2021.01.031.

[6] S. Biswas, B. C. Ray, Preparation of economically viable and environment friendly composites from effluents of aleuritic acid industry, *Journal of Polymers and the Environment*, 2013, **21**, 1026-1031, doi: 10.1007/s10924-013-0606-y.

[7] S. Limmatvapirat, C. Limmatvapirat, M. Luangtana-Anan, J. Nunthanid, T. Oguchi, Y. Tozuka, K. Yamamoto, S. Puttipipatkhachorn, Modification of physicochemical and mechanical properties of shellac by partial hydrolysis, *International Journal of Pharmaceutics*, 2004, **278**, 41-49, doi: 10.1016/j.ijpharm.2004.02.030.

[8] M. Ali, D.K. Hazra, H. Naiya, K.K. Sharma, A. Mohanasundaram, Microwave-assisted extraction and purification of aleuritic acid from seedlac: A fast, eco-friendly and cost-effective single process for enhanced yield and purity, *Chemical Engineering and Processing-Process Intensification*, 2024, **197**, 109716, doi: 10.1016/j.cep.2024.109716.

[9] D. Zhang, B. Zhang, L. Zhu, A new method for shellac binder detection in ancient building mortars, *New Journal of Chemistry*, 2022, **46**, 7563-7568, doi: 10.1039/D2NJ00016D.

[10] P. Zhang, Q. Feng, Research progress of lac waste water treatment, *New Chemical Materials*, 2020, **48**, 263-266, doi:10.19817/j.cnki.issn1006-3536.2020.02.057.

[11] Y. Chen, Z. Zhu, K. Shi, Z. Jiang, C. Guan, L. Zhang, T. Yang, F. Xie, Shellac-based materials: Structures, properties, and applications, *International Journal of Biological Macromolecules*, 2024, **279**, 135102, doi: 10.1016/j.ijbiomac.2024.135102.

[12] B. Saberi, S. Chockchaisawasdee, J. B. Golding, C. J. Scarlett, C. E. Stathopoulos, Development of biocomposite films incorporated with different amounts of shellac, emulsifier, and surfactant, *Food Hydrocolloids*, 2017, **72**, 174-184, doi: 10.1016/j.foodhyd.2017.05.042.

[13] L. Liu, X. Li, K. Li, C. Feng, Z. Gao, J. Ma, J. Xu, H. Zhang, Synthesis of broad-spectrum tunable photoluminescent organosilicon nanodots from lac dye for cell imaging, *Dyes and Pigments*, 2023, **212**, 111090, doi: 10.1016/j.dyepig.2023.111090.

[14] S. Kumar, A. Sharma, L. Cherwoo, N. Thombare, A. P.

Bhondekar, DFT study on the polymerization mechanism of aleuritic acid and jalaric acid in shellac molecule, *Kuwait Journal of Science*, 2024, **51**, 100138, doi: 10.1016/j.kjs.2023.10.005.
[15] J. Lu, H. Wang, J. Huang, G. Li, Q. Wang, W. Xu, Y. Chen, K. Zhang, J. Wang, Sesquiterpene acids from Shellac and their bioactivities evaluation, *Fitoterapia*, 2014, **97**, 64-70, doi: 10.1016/j.fitote.2014.05.014.
[16] M. P. Colombini, I. Bonaduce, G. Gautier, Molecular pattern recognition of fresh and aged shellac, *Chromatographia*, 2003, **58**, 357-364, doi: 10.1365/s10337-003-0037-3.
[17] J. Lu, L. Shang, H. Wen, J. Huang, G. Li, J. Wang, Structural identification and biological activity of six new Shellolic esters from Lac, *Fitoterapia*, 2018, **125**, 221-226, doi: 10.1016/j.fitote.2017.11.021.
[18] J. Li, W. Li, Z. Ye, Y. Sun, W. Gong, Y. Wang, Y. Bi, Determination of hydroxyl value of vegetable oils-based polyols through ring-preopening, solvent-extraction, and acetylation method, *Journal of the American Oil Chemists' Society*, 2024, **101**, 1343-1355, doi: 10.1002/aocs.12842.
[19] W. Ding, J. Zhou, Y. Zeng, Y. Wang, B. Shi, Preparation of oxidized sodium alginate with different molecular weights and its application for crosslinking collagen fiber, *Carbohydrate Polymers*, 2017, **157**, 1650-1656, doi: 10.1016/j.carbpol.2016.11.045.
[20] X. Pan, Y. Tian, J. Li, Q. Tan, J. Ren, Bio-based polyurethane reactive hot-melt adhesives derived from isosorbide-based polyester polyols with different carbon chain lengths, *Chemical Engineering Science*, 2022, **264**, 118152, doi: 10.1016/j.ces.2022.118152.
[21] L. Nasseri, C. Rosenfeld, P. Solt-Rindler, R. Mitter, J. Moser, A. Kandelbauer, J. Konnerth, H. W. Van Herwijnen, Comparison between cure kinetics by means of dynamic rheology and DSC of formaldehyde-based wood adhesives, *Journal of Adhesion*, 2024, **101**, 1-22, doi: 10.1080/00218464.2023.2300453.
[22] H. Yu, Y. Xia, X. Liu, H. Chen, Z. Jin, Z. Wang, S. Wang, Preparation of self-assembled modified reed fiber reinforced starch-based adhesive and the study of cross-linking mechanism, *Industrial Crops and Products*, 2024, **211**, 118204, doi: 10.1016/j.indcrop.2024.118204.
[23] S. Abe, T. Oguma, T. Asaoka, Flow pattern determination and rheological characteristics of high-density phase change material slurry in homogeneous flow, *Chemical Engineering Science*, 2024, **283**, 119362, doi: 10.1016/j.ces.2023.119362.
[24] G. E. Cunningham, F. Alberini, M. J. Simmons, J. J. O'sullivan, Understanding the effects of processing conditions on the formation of lamellar gel networks using a rheological approach, *Chemical Engineering Science*, 2021, **242**, 116752, doi: 10.1016/j.ces.2021.116752.
[25] J. Wang, Y. Bi, J. Liang, Z. Lu, K. Liu, Y. Liu, C. Jiang, Z. Yu, K. Zhang, X. Peng, Atmospheric moisture-digesting zwitterionic skin for non-drying and self-adhesive multifunctional electronics, *Nano Energy*, 2024, **124**, 109500, doi: 10.1016/j.nanoen.2024.109500.
[26] A. Ahuja, V. K. Rastogi, Physicochemical and thermal characterization of the edible shellac films incorporated with oleic acid to enhance flexibility, water barrier and retard aging, *International Journal of Biological Macromolecules*, 2024, **269**, 132136, doi: 10.1016/j.ijbiomac.2024.132136.
[27] A. Ahuja, A. Singh, V. K. Rastogi, Thermal crosslinking kinetics of shellac and its coating for stiffened and water stable cellulose-based paper straws, *International Journal of Biological Macromolecules*, 2024, **278**, 135076, doi: 10.1016/j.ijbiomac.2024.135076.
[28] S. Sen, C. Dong, A. I. D'Aquino, A. C. Yu, E. A. Appel, Biomimetic non-ergodic aging by dynamic-to-covalent transitions in physical hydrogels, *ACS Applied Materials & Interfaces*, 2024, **16**, 32599-32610, doi: 10.1021/acsami.4c03303.
[29] Q. Yue, S. Wang, S. T. Jones, L. A. Fielding, Multifunctional self-assembled block copolymer/iron oxide nanocomposite hydrogels formed from wormlike micelles, *ACS Applied Materials & Interfaces*, 2024, **16**, 21197-21209, doi: 10.1021/acsami.4c03007.
[30] R. M. Daoub, A. H. Elmubarak, M. Misran, E. A. Hassan, M. E. Osman, Characterization and functional properties of some natural Acacia gums, *Journal of the Saudi Society of Agricultural Sciences*, 2018, **17**, 241-249, doi: 10.1016/j.jssas.2016.05.002.
[31] A. H. Shah, X. Li, X. Xu, A. Q. Dayo, W. Liu, J. Bai, J. Wang, Evaluation of mechanical and thermal properties of modified epoxy resin by using acacia catechu particles, *Materials Chemistry and Physics*, 2019, **225**, 239-246, doi: 10.1016/j.matchemphys.2018.12.063.
[32] T. Xu, R. Fu, Determination of effective diffusion coefficient and interfacial mass transfer coefficient of bovine serum albumin (BSA) adsorption into porous polyethylene membrane by microscope FTIR-mapping study, *Chemical Engineering Science*, 2004, **59**, 4569-4574, doi: 10.1016/j.ces.2004.07.024.
[33] L. Liu, G. Yi, K. Li, J. Ma, J. Xu, W. Zhang, Y. Sun, H. Zhang, Synthesis of carbon quantum dots from lac dye for silicon dioxide imaging and highly sensitive ethanol detecting, *Dyes and Pigments*, 2019, **171**, 107681, doi: 10.1016/j.dyepig.2019.107681.
[34] T. Sasaki, S. Hashimoto, N. Nogami, Y. Sugiyama, M. Mori, Y. Naka, K.V. Le, Dismantlable thermosetting adhesives composed of a cross-linkable poly (olefin sulfone) with a photobase generator, *ACS Applied Materials & Interfaces*, 2016, **8**, 5580-5585, doi: 10.1021/acsami.5b10110.
[35] M. Winiecki, P. Krawczyk, Titanium-peroxy and peroxide complex functionalities on Ti-6Al-4V alloy effected by

modification with active radicals, *Chemical Engineering Science*, 2021, **237**, 116543, doi: 10.1016/j.ces.2021.116543.
[36] H. Chen, X. Liu, Q. He, S. Zhang, S. Xu, Y. Wang, Upcycling Waste Thermosetting Polyimide Resins into High-performance and Sustainable Low-temperature-resistance Adhesives, *Advanced Materials*, 2024, **36**, 2310779, doi: 10.1002/adma.202310779.
[37] S. Huang, Y. Wan, X. Ming, J. Zhou, M. Zhou, H. Chen, Q. Zhang, S. Zhu, Adhering low surface energy materials without surface pretreatment via ion-dipole interactions, *ACS Applied Materials & Interfaces*, 2021, **13**, 41112-41119, doi: 10.1021/acsami.1c11822.
[38] X. Huang, C. Ding, Y. Wang, S. Zhang, X. Duan, H. Ji, Dual dynamic cross-linked epoxy vitrimers used for strong, detachable, and reworkable adhesives, *ACS Applied Materials & Interfaces*, 2024, **16**, 38586-38605, doi: 10.1021/acsami.4c08123.
[39] R. Hensel, J. Thiemecke, J. A. Booth, Preventing catastrophic failure of microfibrillar adhesives in compliant systems based on statistical analysis of adhesive strength, *ACS Applied Materials & Interfaces*, 2021, **13**, 19422-19429, doi: 10.1021/acsami.1c00978.
[40] Z. Zhao, P. Zhao, Y. Zhao, J. Zuo, C. Li, An underwater long-term strong adhesive based on boronic esters with enhanced hydrolytic stability, *Advanced Functional Materials*, 2022, **32**, 2201959, doi: 10.1002/adfm.202201959.
[41] J. Ren, G. Du, S. Liu, H. Yang, X. Ran, C. Liu, T. Liu, Z. Li, X. Zhou, W. Gao, High-strength, self-initiated, wide pH range of underwater adhesive suitable for different severe environments, *Chemical Engineering Journal*, 2023, **455**, 140640, doi: 10.1016/j.cej.2022.140640.
[42] Z. Wang, Y. Wang, H. Wang, H. Gang, N. Zhang, Y. Zhou, S. Gu, Y. Zhuang, W. Xu, G. Ke, Bioinspired natural magnolol-based adhesive with strong adhesion and antibacterial properties for application in wet and dry environments, *ACS Applied Materials & Interfaces*, 2023, **15**, 24846-24857, doi: 10.1021/acsami.3c02136.
[43] B. Zhang, P. Zhang, G. Zhang, C. Ma, G. Zhang, Sterically hindered oleogel-based underwater adhesive enabled by mesh-tailoring strategy, *Advanced Materials*, 2024, **36**, 2313495, doi: 10.1002/adma.202313495.